International Journal of Astrobiology 5 (4): 307–312 (2006) Printed in the United Kingdom
doi:10.1017/S1473550406003089 First published online 23 November 2006

Meteoroids: a landing capsule for panspermia

S.G. Coulson

Centre for Astrobiology, School of Mathematics, Cardiff University, 2 North Road, CF2 4HY, UK
e-mail: coulson@aldpartners.com

Abstract: Viable, organic material has been discovered at altitudes of around 40 km above the Earth (Wainwright *et al*. (2004). *Int J. Astrobiol*. **3**(1), 13–15). Assuming an extraterrestrial origin, this raises the question of how the material survived air breaking in the atmosphere from hypervelocity speeds. The Earth is under constant bombardment from interplanetary and interstellar dust particles, with a daily influx of over 60 tonnes of material incident upon the upper atmosphere. The majority of this material is in the form of micro-meteoroids with typical radii ranging from 0.01 μm to a peak of around 200 μm (Ceplecha *et al*. (1998). *Space Sci. Rev*. **84**, 327–471).

Classical work on meteoroid ablation suggests that these particles should be annihilated by atmospheric deceleration. Recent work suggests that molecular sputtering of surface molecules may provide an alternative way to decelerate, without such intense heating. In general, the mathematics of atmospheric entry are complex; here we review some of the main parameters (particle size, initial velocity, entry angle and composition) that contribute to the heating of meteoroids during their descent. Comparing the heating profiles for meteoroids descending from inside and outside of the Earth's shadow, it is found that the maximum temperatures reached by 10 μm meteoroids can be 10–15% lower if the meteoroid descends from within the shadow of the Earth, compared to those decelerating during daylight. The possibility that micrometre-sized particles can decelerate subject to maximum temperatures ~300 K offers a mechanism for the survivability of the recovered organic material.

Received 26 June 2006, accepted 28 June 2006

Key words: asteroids, comets, meteors, meteoroids, panspermia.

Introduction

Over the last century it had become almost axiomatic to view the Earth as a closed system, existing independently from the rest of the universe. From this axiom, the existence of life is postulated to have begun on the Earth and its evolution to be contained within the Earth's biosphere. The theory of panspermia (e.g. for recent discussions see Hoyle & Wickramasinghe (1991); Burchell (2004)) challenges this view by proposing that life is widespread throughout the universe and that it can be spread, by the migration of comets and asteroids, between planets and throughout galaxies. Napier (2004) and Wallis & Wickramasinghe (2004) have recently reviewed the arguments for interstellar panspermia, and Melosh (2003) provides an alternative view that offers arguments against the interstellar hypothesis.

The discovery of Martian meteorites demonstrates that the transfer of fragments from one planet to the surface of another is a viable process (Mileikowsky *et al*. 2000; Melosh 1988). Describing the mechanisms by which viable micro-organisms can survive the rigors of interplanetary displacement is the main challenge towards developing the theory of panspermia. The interplanetary environment is inhospitable for bacterial life, with large variations in temperature and high radiation doses (Clark *et al*. 1999); however, bacteria on Earth have shown their hardiness in withstanding extremes of temperature ranging from polar ice to volcanic craters. Sufficient shielding from Solar radiation may be provided by a protective skin of charred material: a thin outer layer of carbon radically alters the optical properties of a body, so that a greater proportion of the incident radiation is reflected.

As harsh as the journey through space is, it is the final 100 km or so of an interplanetary grain's journey to the surface of the Earth that poses the greatest challenge to the survivability of viable bacteria. Meteoroids enter the Earth's atmosphere with hypervelocity speeds between 11.2–72 km s^{-1} and are rapidly decelerated within time-scales of a few seconds to settling speeds of a few cm s^{-1}. These high decelerations produce extreme pressure and heating on meteoroids. As potential carriers of life, meteoroids act as a form of landing capsule for microorganisms, an understanding of their dynamics and temperature profiles within the Earth's atmosphere is vital to the theory of panspermia. Earlier work (Coulson 2002; Coulson & Wickramasinghe 2003) has examined the atmospheric air breaking of micrometre-sized meteoroids by sputtering with air molecules. It was found that particles with radii ~10 μm reach maximum temperatures of ~500 K. Here we examine

the general problem of atmospheric entry and the difference in the maximum temperature between meteoroids that enter the atmosphere from the Earth's shadow and those from the daylight side.

The flux of organic material at the Earth's upper atmosphere

On an average day approximately 65 tonnes of matter enter the Earth's upper atmosphere (see Coulson (2004) for a review), most of this is in the form of Interplanetary Dust Particles (IDPs) with radii ranging from 0.1–100 μm. From the analysis of micrometre-sized meteoroids recovered from space or by high altitude aircraft, Brownlee (1978) was able to determine their origin from their composition and structure. It was found that meteoroids from cometary sources were typically of porous, aggregate compositions with relatively low densities. Meteoroids from asteroidal sources had closer packed structures with higher densities.

The particles discovered by Brownlee were typically ~1–10 μm in diameter. Laboratory analysis of these particles has revealed details of their structure and composition. Around 60% of the samples obtained by Brownlee (1985) were made up of chrondritic material. These particles were mostly in the form of compact grains, but some occurred as porous structures, where volatile material such as ices may have been boiled off either in free space or ablated during the particle's deceleration in the atmosphere. Of the particles examined 30% were iron–sulphur–nickel. These were found as single particles, with chrondritic material adhering to their surface or as particles embedded in larger chrondritic fragments. The remainder of the particles sampled were made from mafic silicate.

The collection of these particles by an aircraft travelling with speeds ~960 km h^{-1} may have caused significant damage to their fine structure. The balloon experiment, described by Wickramasinghe *et al*. (2003), took samples of the atmosphere at much lower relative speeds and was able to recover a greater proportion of porous material. In their experiments, Wickramasinghe *et al*. (2003) detected viable, but non-cultureable bacteria, and were able to culture two bacteria and a fungus from the stratosphere at an altitude of 41 km. Extrapolating from the results of the experiment suggests an in-fall rate of ~3 tonnes per day of viable bacteria (cultureable and non-cultureable). This implies that around 4.6% of all IDPs incident upon the Earth are in the form of viable bacteria.

Meteoroid dynamics

The path of an interplanetary dust particle, of mass m, approaching the Earth from free space can be described by the gravitational Hamiltonian

$$H(q,\dot{q}) = \frac{1}{2}m\dot{q}\dot{q} + \frac{m\mu}{q} \tag{1}$$

where μ is the gravitational potential of the Earth and q, $\dot{q}$ are generalised position and velocity co-ordinates, assuming that the only potential influencing the motion of the particle is the gravitational attraction of the Earth.

Equation (1) is only valid when the meteoroid body is outside the Earth's atmosphere; upon entering the atmosphere energy is no longer conserved as the body loses kinetic energy due to atmospheric drag. This kinetic energy goes into heating the meteoroid and the surrounding atmosphere. The equation of motion for an object of mass m falling through the Earth's atmosphere under the influence of gravity is given by the equation

$$m\frac{d^2r}{dt^2} = \frac{m\mu}{r^2} - S\Gamma(V)\rho_a \tag{2}$$

where V is the velocity of the meteoroid, r is the geocentric distance, S is the cross-sectional area of the object, ρ_a is the atmospheric density and Γ the drag coefficient which may be a function of V or V^2 (Coulson 2002).

Using geocentric, polar coordinates in an inertial frame of reference, Equation (2) can be resolved in the radial and transverse directions

$$m(\ddot{r} - r\dot{\theta}^2) = \frac{m\mu}{r^2} - S\Gamma(V)\rho_a \sin\alpha, \tag{3}$$

$$m\frac{1}{r}\frac{d}{dt}\left(r^2\dot{\theta}\right) = -S\Gamma(V)\rho_a \cos\alpha, \tag{4}$$

where α is the flight angle such that

$$\tan\alpha = \frac{1}{r}\frac{dr}{d\theta}$$

and

$$V^2 = \dot{r}^2 + r^2\dot{\theta}.$$

As the meteoroid traverses the atmosphere it is initially heated by direct collisions with the air molecules at altitudes of typically greater than 100 km. With entry velocities greater than 10 km s^{-1}, this initial heating has a very short duration of the order of a few seconds. The heat transfer for small meteoroids with radii less than 1 mm is dominated by radiative processes and is outlined in the following section. For particles with radii greater than 1 mm, the heat transfer process is essentially one of conduction. Typical skin depths mean that the outer layers of the meteoroid are only heated to a maximum of a few millimetres below the surface within the timescale of direct heating (Sears 1975).

Heating of the meteoroid by direct impact causes it to lose mass by fragmentation and, as the temperature rises, evaporation and melting of its surface. The majority of the kinetic energy of a meteoroid is dissipated by these processes, which are collectively known as ablation. Analytical descriptions of the ablation process are complicated by the fragmentation of the meteoroid. Fragmentation is difficult to describe as it may occur as a continuous process or as a discrete number of one or more events (Foschini 2001).

Classical meteoroid theory (Bronshten 1983) makes the assumption that ablation is a continuous process; the mass

https://doi.org/10.1017/S1473550406003089 Published online by Cambridge University Press

loss equation for a meteoroid is given by the equation

$$\frac{dm}{dt} = -\frac{\Lambda}{2Q} S\rho_a V^3 \tag{5}$$

where Λ is the coefficient of heat transfer between the atmosphere and the meteoroid and Q is the latent heat of vaporization for the meteoroid.

A meteoroid falling through the atmosphere experiences a pressure across its leading face, due to the aerodynamic loading or ram pressure P_{ram} of the air. As the evaporation of molecules from the surface of the meteoroid increases, a vapour cloud starts to form around the meteoroid. From Equation (5), the pressure exerted by the vapour is proportional to V^5. For high-velocity meteoroids, the pressure exerted by the vapour is greater than the ram pressure and the vapour cloud screens the meteor from direct collisions with the air molecules (Popova *et al.* 2000).

For a meteoroid travelling at a velocity of around 70 km s^{-1} with a radius $\sim$10 cm, the ram pressure exceeds the vapour pressure at an altitude of around 90 km. So, at altitudes less than 90 km, the pressure acting on the meteoroid is effectively that of the ram pressure.

A meteoroid will fragment when the ram pressure, P_{ram}, is equal to the maximum tensile strength of the meteor (Hills & Goda 1993). From Equation (2)

$$P_{ram} \approx \rho_a V^2. \tag{6}$$

The fragmentation and ablation relationships, Equations (5) and (6) respectively, suggest that the cross-sectional area of the meteoroid is also dependent on the altitude of the meteoroid

$$S' = S(r, \theta, \alpha), \tag{7}$$

Bronshten (1983) models the variation in cross-section by the use of a standard shape variation parameter β with a mass power law. For a body with initial cross-section S_0 and initial mass m_0, the variation in cross-section is given by the following equation:

$$S = S_0 \left(\frac{m}{m_0}\right)^{\beta}. \tag{8}$$

The atmospheric density, ρ_a, is normally taken as an exponentially decreasing function of altitude,

$$\rho_a = \rho_0 e^{-ar} \tag{9}$$

for constants ρ_0 and a.

The atmospheric form taken in Equation (9) is the derived by assuming that the atmosphere is an ideal gas, obeying the well-known relation

$$PV = nRT.$$

Combining this with the hydrostatic equation

$$\frac{dP}{dr} = -\rho g$$

and integrating one obtains

$$\rho_a = \rho_0 e^{gh/RTH} \tag{10}$$

where h is the altitude and H is the scale height (Allen 2000), so that the atmospheric density varies as $e^{1/T}$. Most models of meteoroid descent (Nicol *et al.* 1985; Love & Brownlee 1993) treat the temperature of the stratosphere as a constant; however, meteoroids with a radii of greater than 100 μm attain high temperatures of above 1000 K in the atmosphere. In general, the detailed atmospheric response to the transit of a very hot meteoroid body is a complicated, non-equilibrium problem. Briefly stated, the effect of temperature response in reducing the local atmospheric density in front of the path of a meteoroid is significant for large meteoroid bodies that attain high temperatures. This may be the reason why some large meteoroids have been observed at lower heights than expected before total ablation occurs.

To obtain analytical solutions for the equations of motion of the meteoroid, the series of Equations (3)–(5), (9) and (10) must be solved simultaneously. The highly non-linear form of these equations means that general, closed, analytical solutions do not exist.

In order to obtain solutions to the general problem of an ablating, meteoroid body falling through a stratified atmosphere, simplifications to the equations need to be made. For an exo-atmospheric meteoroid the motion is Keplerian with well-known closed solutions. Making the assumption that, for non-massive meteoroids at relatively low altitudes, the atmospheric drag is the dominant force on the body enables closed solutions to be obtained at the low-altitude limit by using the method of matched asymptotic expansions. Other assumptions such as constant ablation of a body that remains spherical allow analytical solutions to be obtained (Coulson 2003).

Temperature difference in atmospheric descents during day and night

Another simplification to the series of equations governing meteoroids in the atmosphere is to treat gravity as a constant. At an altitude of 100 km, the acceleration due to gravity is still $\sim$97% of that at sea-level, so for small meteoroids the approximation is valid. Making this assumption, Coulson & Wickramasinghe (2003) derived an expression for the variation of temperature with altitude for 0.1–10 μm meteoroid grains. A key assumption in this derivation was the temperature of these grains prior to their descent through the atmosphere.

By considering the radiation absorption and re-emission at a Solar distance of 1 AU, equilibrium temperatures for grains ranging in size from 0.001–100 μm were calculated. For grains greater than 10 μm the size of the grain was greater than the wavelength of the incident ultraviolet/visible radiation (typically 0.2–0.8 μm) and of the emitted infrared (typically 2–12 μm). A grain in thermal equilibrium, at a temperature of 1000 K, has a peak emission wavelength

https://doi.org/10.1017/S1473550406003089 Published online by Cambridge University Press

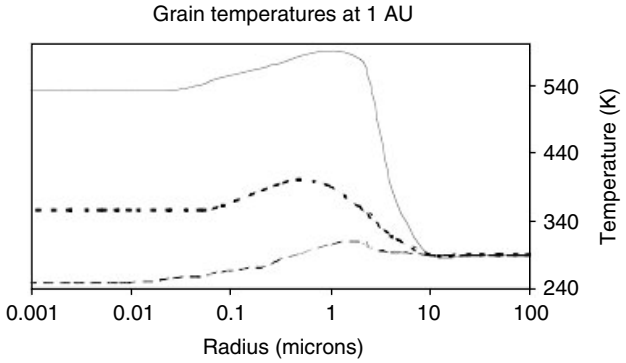

Fig. 1. Equilibrium grain temperatures at 1 AU from the Sun (Coulson & Wickramasinghe 2003). The solid line represents grains composed of an idealised grey-body material $m = 1.4 - 0.1i$. The dashed line is for grains made from a dielectric material, and the middle line grains composed of an organic material.

$\sim$3 μm. This allows grains $\sim$10 μm to be treat as black bodies with respect to their emission and absorption, so rate of emission of thermal radiation is proportional to T^4. As shown in Fig. 1, these grains have an equilibrium temperature of around 289 K, at a Solar distance of 1 AU. For particles with radii comparable to the wavelengths of the incident and emitted radiation the evaluation of the absorption and scattering coefficients is complicated by scattering effects, and the Mie Scattering relations are required (Coulson & Wickramasinghe 2003).

The equilibrium grain temperatures at a distance of 1 AU from the Sun for different particle radii and materials are summarized in Fig. 1. This shows that the temperature difference between large and small particles of a given material is large at a heliocentric distance of 1 AU. Ideal grey-body grains smaller than 10 μm have higher equilibrium temperatures than larger grains, as they are unable to emit sufficient energy at lower temperatures. For a fixed grain composition, the smallest sub-micrometre grains are at lower equilibrium temperatures than grains with radii of around 1 μm, due to the fact that the smaller grains are less efficient emitters of infrared wavelengths that are of the same order of magnitude as the grain radii.

For real grain materials (as opposed to ideal grey-body grains) equilibrium grain temperatures are dependent on the composition as well as the grain radius. The organic particles that are more likely to be found in IDPs than idealized grey-body particles (Hoyle & Wickramasinghe 1999) are typically around 280 K, cooler than idealized grey-body grains, for particle radii greater than or equal to 1 μm. This is due to the fact that organic molecules tend to have low absorption values in the visible wavelengths and high absorption resonances due to C—H, O—H and C═C bond stretching.

Grains that move into the Earth's shadow prior to atmospheric entry will be at temperatures lower than their equilibrium temperature. The temperature of the grain as it starts its descent is determined by the amount of time the grain spends in the shadow of the Earth. Consider a grain of radius

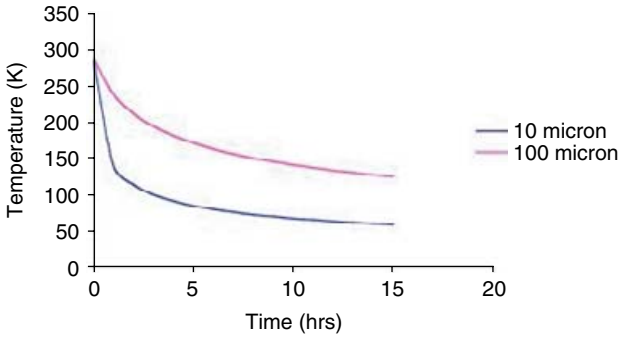

Fig. 2. Grain temperature (K) against time (hours) for 10 and 100 μm spherical, organic grains, with a density of 0.6 g cm^{-3} and specific heat capacity of 1 K g^{-1}.

a, at an equilibrium temperature T_0, the main mechanism for cooling the grain in free space is by the emission of radiation. The radiation emitted per unit time for a grain at temperature T_g is given by the equation

$$4\pi a^2 \int_{\lambda} d\lambda Q_{abs}(\lambda, a)\, B(\lambda, T_g) \tag{11}$$

where Q_{abs} is the absorption cross-section and B is the Planck function at temperature T_g. Hence the rate of cooling of the grain is given by

$$MC_v \frac{dT_g}{dt} = 4\pi a^2 \int_{\lambda} d\lambda Q_{abs}(\lambda, a) B(\lambda, T_g) \tag{12}$$

for a grain of mass M and specific heat capacity C_v.

For grains with radii $\sim$10 μm, the emission of radiation can be approximated as a black body, so that Equation (12) becomes

$$\int_{\lambda} d\lambda Q_{abs}(\lambda, a) B(\lambda, T_g) \approx \sigma T_g^4 \tag{13}$$

where s is the Stefan–Boltzmann constant. Substituting the black body approximation into Equation (12) for a spherical grain of density ρ and integrating gives the grain temperature after time t:

$$T_g = T_0 \left\{ \frac{1}{1 + (9\sigma t T_0^3 / a\rho C_v)} \right\}^{1/3} \tag{14}$$

Fig. 2 plots the fall in temperature over time for 10 μm grains composed of organic material, the $t^{-1/3}$ relation means that the rate of cooling is initially high and decreases over time. Cooling for 0.1–1 μm grains is derived in a similar fashion to Equation (13) but the temperature decreases as $t^{-1/4}$, as radiation emission is proportional to T^5 for grains in the Mie Scattering region. The cooling curves for 0.1–1 μm grains are shown in Fig. 3; the rate of cooling is greater for grains smaller than 1 μm as compared with larger grains.

For grains with equilibrium temperatures less than 300 K, partially composed of volatile, icy material, energy is lost from the grain by sublimation as well as by radiation emission.

https://doi.org/10.1017/S1473550406003089 Published online by Cambridge University Press

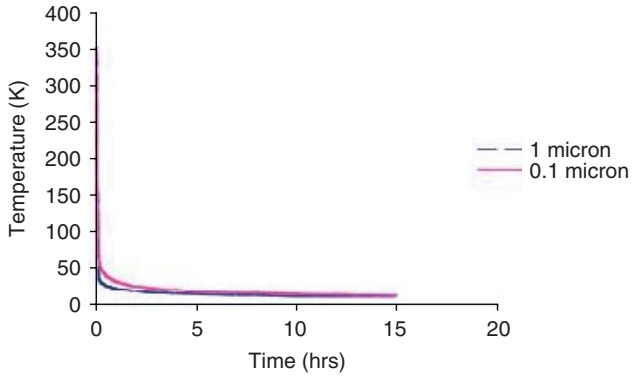

Fig. 3. Grain temperature (K) against time (hours) for 1 and 0.1 μm spherical, organic grains, with a density of 0.6 g cm^{-3} and specific heat capacity of 1 K g^{-1}.

To allow for this, the grain cooling equation (Equation (12)) needs an additional term on the right-hand side. If the grain has a mass m and H is the enthalpy of phase change then we have the following equation:

$$MC_{\mathrm{v}}\frac{dT_{\mathrm{g}}}{dt}=4\pi a^{2}\int_{\lambda}d\lambda Q_{\mathrm{abs}}(\lambda,a)B(\lambda,T_{\mathrm{g}})+\frac{1}{4}H\frac{dm}{dt} \qquad (15)$$

This assumes that H is the enthalpy change for both sublimation and vaporization. For grains in free space, the pressure from the sublimating molecules is very low and localized around the grain. Several laboratory studies have shown that sublimating mixtures (both salts and organics) do not simply evaporate, but grow complex structures (Wallis & Al-Mufti 1996). The localized pressure of sublimating material can be an important parameter in the formation of this material.

Wallis *et al*. (1987) calculated lifetimes of grains comprised of ice with graphite impurities, evaporated from the coma of P/Halley at times $t<100$ s, the precise value being dependent on the impurity content. Sub-micrometre grains with radii of 0.3 μm and 0.1 μm composed of the same material had lower lifetimes of $t<10$ s, at the same Solar distance of 1 AU.

From Fig. 1, grains composed of organic materials have equilibrium temperatures less than 300 K so that radiative cooling rather than sublimation is the dominant mechanism. From Equation (13) grains composed of idealized grey body or dielectric material cool to temperatures less than 300 K within timescales of the order of 10 s, so sub-micrometre grains made from these materials are not expected to survive the cooling process.

Conclusion

Overall, the general problem of a meteoroid descending through the atmosphere depends strongly on its physical properties such as density and refractive index. The samples recovered from the upper atmosphere suggest that meteoroids are typically porous and highly irregular in shape. There is a need for accurate data on these physical properties, of organic grains both prior to and after atmospheric deceleration, to improve current dynamic models.

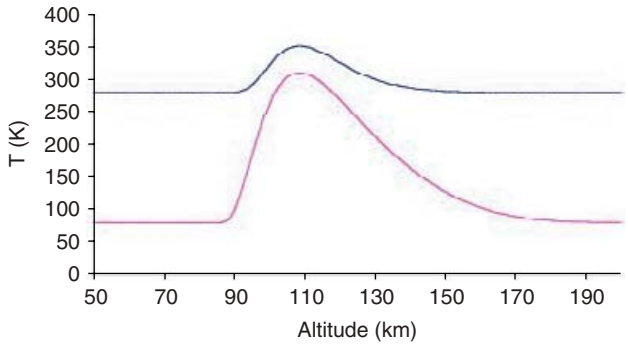

Fig. 4. Daylight (top) and night temperature profiles for 10 μm particles with a density of 0.6 g cm^{-3}, an initial velocity of 12 km s^{-1} and an entry angle of 45°. The particles were assumed to be slowed by sputtering, with relatively low sputtering coefficient of 0.5.

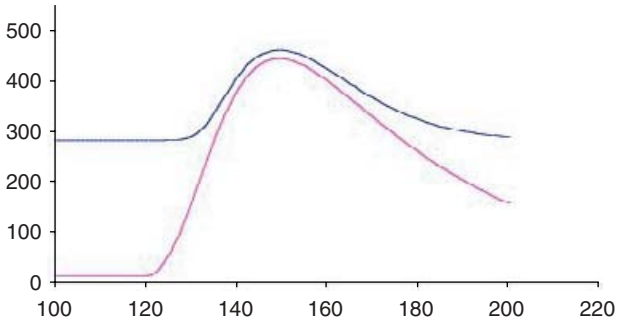

Fig. 5. Daylight (top) and night temperature profiles for 1.0 μm particles with a density of 0.6 g cm^{-3}, an initial velocity of 12 km s^{-1} and an entry angle of 45°. The particles were assumed to be slowed by sputtering, with relatively low sputtering coefficient of 0.5.

The Meteoroid Dynamics section demonstrated that the dynamics of a meteoroid as it enters the Earth's atmosphere are highly sensitive to its initial conditions. Changes to the meteoroid affect all of the equations governing its subsequent motion within the atmosphere; it was found that the presence of a hot meteoroid body reduces the effective density of the atmosphere through which it passes.

After cooling in the Earth's shadow for 5 h a 10 μm grain will be at a temperature of approximately 86 K, and a 1 μm grain will be at a temperature of 15 K. The temperature profiles of 10 and 1 μm grains composed of an organic material are shown for daylight descent (Figs 4 and 5, respectively). If these grains were to descend after cooling for 5 h in the Earth's shadow, the 10 μm grain would reach a maximum temperature of between 300 and 320 K, depending on the sputtering coefficient. So a night time descent of a 10 μm meteoroid can be between 10–15% cooler than atmospheric entry during daylight. Meteoroid grains with 1 μm radii are heated to much higher temperatures, so the difference between nocturnal and daytime entry only

https://doi.org/10.1017/S1473550406003089 Published online by Cambridge University Press

equates to a reduction to the maximum temperature of around 1–5%.

Meteoroids of 10 μm entering the atmosphere from the Earth's shadow are subjected to significantly more benign temperatures than identical meteoroids that are decelerated during daylight. The fact that these particles can be retarded to settling speeds without excessive heating suggests a mechanism for the survival of the porous, organic particles discovered by Wickramasinghe *et al*. (2003).

References

Allen, C.W. (2000). *Astrophysical Quantities*. Athlone, London.

Bronshten, V.A. (1983). *Physics of Meteoric Phenomena*. Reidel, Dordrecht.

Brownlee, D.E. (1978). In *Cosmic Dust*, ed McDonnell J.A.M. Wiley, New York.

Burchell, M.J. (2004). *Int. J. Astrobiol*. **3(2)**, 73–80.

Ceplecha, Z., Borovicka, J., Elford, G.W., ReVelle, D.O., Hawkes, R.L., Porubcan, V. & Simek, M. (1998). *Space Sci. Rev*. **84**, 327–471.

Clark, B.C., Baker, A.L., Cheng, A.F., Clemett, S.J., McKay, D., McSween, H.Y., Pieters, C.M., Thomas, P. & Zolensky, M. (1999). *Orig. Life Evol. Biosph*. **29**, 521–545.

Coulson, S.G. (2002). *Mon. Not. R. Astron. Soc*. **332**, 741–744.

Coulson, S.G. (2003). *Astrophys. Space Sci*. **283**, 275–281.

Coulson, S.G. (2004). *Int. J. Astrobiol*. **3(2)**, 151–156.

Coulson, S.G. & Wickramasinghe, N.C. (2003). *Mon. Not. R. Astron. Soc*. **343**, 1123–1130.

Foschini, L. (2001). *Astron. Astrophys*. **365**, 612–621.

Hills, J.G. & Goda, M.P. (1993). *Astron. J*. **105(3)**, 1114–1144.

Hoyle, F. & Wickramasinghe, N.C. (1991). *The Theory of Cosmic Grains*. Kulwer, Dordrecht.

Love, S.G. & Brownlee, D.E. (1993). *Science* **262**, 550–553.

Mileikowsky, C. *et al*. (2000). *Icarus* **145**, 391–427.

Melosh, H.J. (1988). *Nature* **332**, 687–688.

Melosh, H.J. (2003). *Astrobiology* **3**, 207–215.

Nicol, E.J., Macfarlane, J. & Hawkes, R.L. (1985). *Planet. Space Sci*. **3**, 315.

Popova, O.P., Sidneva, S.N., Shuvalov, V.V. & Strelkov, A.S. (2000). *Earth Moon and Planets* **82–83**, 109–128.

Sears, D.W. (1975). *Modern Geology* **5**, 155–164.

Wainwright, M., Wickramasinghe, N.C., Narlikar, J.V., Rajaratnam P. & Perkins, J. (2004). *Int J. Astrobiol*. **3(1)**, 13–15.

Wallis, M.K. & Al-Mufti, S. (1996). *Earth, Moon and Planets* **72**, 91–97.

Wallis, M.K. & Wickramasinghe, N.C. (2004). *Mon. Not. R. Astron. Soc*. **348**, 52–61.

Wallis, M.K., Rabilizirov, R. & Wickramasinghe, N.C. (1987). *Astron. Astrophys*. **187**, 801.

Wickramasinghe, N.C., Wainwright, M., Narlikar, J.V., Rajaratnam, P., Harris, M.J. & Lloyd, D. (2003). *Astrophysics & Space Science* **283**, 403–413.